FULL PAPER

Dalton
www.rsc.org/dalton

Study of binary and ternary metal complexes containing the sulfato ligand: molecular models for selected non-catalytic sites in sulfurylase†

Gabriella Tamasi and Renzo Cini*

Department of Chemical and Biosystem Sciences and Technologies, University of Siena, Via Aldo Moro 2, I-53100 Siena, Italy. E-mail: cini@unisi.it

Received 11th March 2003, Accepted 23rd May 2003
First published as an Advance Article on the web 12th June 2003

$[Cd^{II}(\mu_2\text{-}O^2,O',O''\text{-}SO_4)(terpy)]_2\cdot 2H_2O$, **1**·$2H_2O$ (terpy, 2,2′:6′,2″-terpyridine) was obtained from the reaction of $3CdSO_4\cdot 8H_2O$ with terpy and consists of centrosymmetric dimeric units in which the two $Cd(terpy)^{2+}$ moieties are held together by two tridentate sulfato anions that act as chelators towards the two metal centres, one oxygen being tri-coordinate. This coordination mode for the sulfato ligand has never been reported before in the solid state. $[Zn^{II}(\mu_2\text{-}O,O'\text{-}SO_4)(terpy)]_2\cdot 2H_2O$, **2**·$2H_2O$, was obtained by using $ZnSO_4\cdot 7H_2O$ through a procedure similar to that followed for **1**·$2H_2O$. Semi-empirical quantum mechanics and density functional structure optimisations were performed at the AM1 and Becke3LYP/(6-31G**, S) levels. The computations reproduced well the main features of the $Zn(\mu_2\text{-}O,O'\text{-}SO_4)_2Zn$ unit as found in **2**. A $[Zn(imidazole)_2(O\text{-}OOCCH_3)_2(O\text{-}SO_4)]^{2-}$ model was also optimised as a model for ATP-sulfurylase from *Saccharomices cerevisae*.

Introduction

The sulfate anion is a *macro-nutrient* taken up from drinking water and food, and is important for the biosynthesis of cysteine and other sulfur containing molecules. The reduction of sulfur from oxidation state +6 to −2 takes place usually through a catalytic cascade which involves first sulfurylase enzymes, whereas the hydrolysis of the sulfate ester linkage is carried out by sulfatases. Recently reported X-ray diffraction studies showed that metal ions such as Mg(II), Zn(II), Co(II) and even Cd(II) are, or may be, present in enzyme systems that have the sulfate anion as substrate, and play at least structural or transport roles relevant to the sulfate itself.[1a–d] For instance, the structure of an ATP-sulfurylase from *Saccharomices cerevisiae*, contains metal ions such as Zn(II), Co(II) and Cd(II).[1a] Several metal sites are thought to play a physiological role whereby Ca(II) or Zn(II) or Co(II) ions replace the Cd(II) ion.[1a] One of the cadmium cations is linked to a sulfato anion, to two carboxylato anions and to two histidine moieties (Scheme 1). Of much interest, the effect of Cd(II) exposure on sulfate assimilation in *Saccharomices cerevisiae* leads to a change of the content of several biomolecules.[1e] It should also be noted that metal–phosphato and –thiophosphato interactions related to biological systems have been deeply investigated in aqueous solutions.[1f–h]

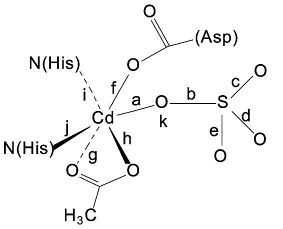

Scheme 1 Drawing of a cadmium site in ATP-sulfurylase from *Saccharomices Cerevisiae* taken from the Protein Data Bank (Deposition Code 1G8F).[32] Selected geometrical parameters are: a, 2.48; b, 1.50; c, 1.45; d, 1.47; e, 1.49; f, 2.16; g, 2.21; h, 2.36; i, 2.37; j, 2.37 Å; k, 141°.

On the other hand, metal–sulfato species have been studied for their important roles in catalysis,[2] in the field of porous-framework materials,[3a] in stabilising Pt(III)–Pt(III) species[3b] and in the chemistry of "*cisplatin*" analogues.[3c] The research works published so far on ternary metal–sulfato–any organic ligand ($M(SO_4)L$) species are several. In fact a search from the Cambridge Crystallographic Data Base (Release November 2002, CCDB)[4] which excludes all the pure inorganic metal–sulfato compounds, listed *ca.* 330 $M(SO_4)L$ compounds with at least a $M\text{–}OSO_3$ linkage. In spite of this, to our knowledge, a systematic analysis of metal–sulfato complexes is still lacking. The coordination modes shown so far by the sulfate are those labelled **I**–**VII** in Scheme 2.

On the basis of this reasoning and as a continuation of a research project devoted to the analysis of the coordination

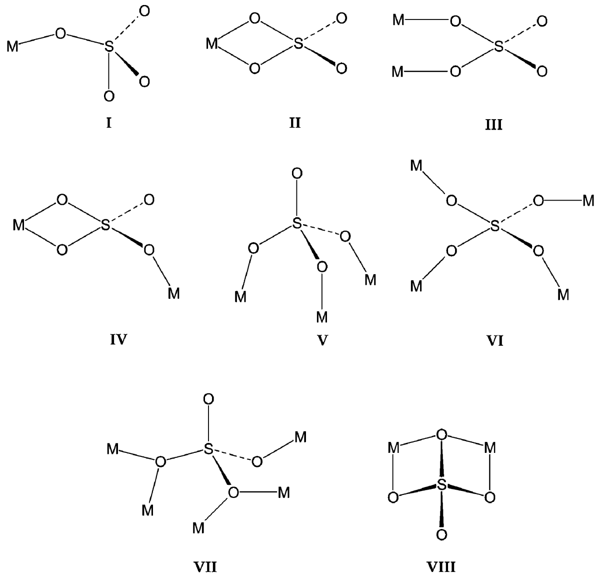

Scheme 2 Coordination modes of sulfate as revealed by X-ray structural studies. Modes **I**–**VII** have been previously reported and deposited at the Cambridge Crystallographic Data Base, November 2002 release.[4] Mode **VIII** has been found for the first time, to our knowledge, in the structure of **1**.

---

† Electronic supplementary information (ESI) available: Full listings of atomic coordinates from X-ray diffraction experiments and from molecular modelling calculations, atomic thermal displacements, bond lengths and bond angles, and computed heat of formation and heat of reaction for selected molecules and reactions, Figure relevant to selected computed structures, and Figure relevant to vibrational modes. See http://www.rsc.org/suppdata/dt/b3/b302779a/

DOI: 10.1039/b302779a

Table 1 Selected crystal data and structure refinement for $[Cd^{II}(\mu_2\text{-}O^2,O',O''\text{–}SO_4)(terpy)]_2\cdot 2H_2O$, **1**·$2H_2O$ and $[Zn^{II}(\mu_2\text{-}O,O'\text{–}SO_4)(terpy)]_2\cdot 2H_2O$, **2**·$2H_2O$

Parameter	**1**·$2H_2O$	**2**·$2H_2O$
Empirical formula	$C_{30}H_{26}Cd_2N_6O_{10}S_2$	$C_{30}H_{26}N_6O_{10}S_2Zn_2$
Formula weight	919.52	825.42
T/K	293(2)	293(2)
λ/Å	0.71073	0.71073
Crystal system	Triclinic	Triclinic
Space group	$P\bar{1}$ (no. 2)	$P\bar{1}$ (no. 2)
Unit cell dimensions		
a/Å	9.079(1)	9.705(1)
b/Å	10.402(1)	9.767(2)
c/Å	10.533(1)	10.322(1)
α/°	119.23(1)	110.14(3)
β/°	105.12(1)	116.62(1)
γ/°	99.54(1)	98.91(1)
V/Å^3	785.66(14)	763.47(19)
Z	2	2
D_c/Mg m^{-3}	1.943	1.795
μ/mm^{-1}	1.556	1.780
Refinement method	Full-matrix least-squares on F^2	Full-matrix least-squares on F^2
Data/restraints/parameters	2545/0/234	2587/0/235
Goodness-of-fit on F^2	1.084	1.060
Final R indices $[I > 2\sigma(I)]$	$R1 = 0.0182$, $wR2 = 0.0441$	$R1 = 0.0302$, $wR2 = 0.0733$
R indices (all data)	$R1 = 0.0214$, $wR2 = 0.0454$	$R1 = 0.0369$, $wR2 = 0.0766$

modes by phosphato[5a,b] and sulfato anions,[5c] we planned the synthesis and structural characterisation of some more sulfato-containing compounds. We wish to report here on $[Cd^{II}(\mu_2\text{-}O^2,O,O'\text{-}SO_4)(terpy)]_2\cdot 2H_2O$, **1**·$2H_2O$ (terpy, 2,2′:6′,2″-terpyridine), and $[Zn^{II}(\mu_2\text{-}O,O'\text{-}SO_4)(terpy)]_2\cdot 2H_2O$, **2**·$2H_2O$. Interestingly, the X-ray diffraction study showed a new co-ordination mode for the SO_4^{2-} ligand for **1** (**VIII**), whereas the coordination pattern for **2** is mode **III**.

Experimental

Materials

Terpy (reagent grade, r.g., Fluka) was recrystallised from EtOH–H_2O 1 · 10 (v/v). $3CdSO_4\cdot 8H_2O$ and $ZnSO_4\cdot 7H_2O$ (analytical grade, a.g., Merck and C. Erba, respectively) were used without any further purification.

Synthesis

$[Cd^{II}(\mu_2\text{-}O^2,O',O''\text{-}SO_4)(terpy)]_2\cdot 2H_2O$, 1·$2H_2O$. A clear solution of terpy (Fluka, 24 mg, 0.103 mmol) in ethanol (95%, 3 mL) was mixed with a clear solution of $3CdSO_4\cdot 8H_2O$ (Merck, 80 mg, 0.104 mmol) in water (6 mL) (1 : 3, terpy : Cd molar ratio). The mixture was heated at 353 K for 10 min and then stored at 293 K. Crystals appeared within 48 h, whereas single crystals suitable for X-ray diffraction analysis formed after 8 weeks. The crystals were filtered off, washed twice with cold water, twice with a few drops of ethanol and then stored at 278 K. Yield, 60%. Anal. Found: C, 38.63; H, 2.51; N, 8.90; S, 6.95. Calc. for $C_{30}H_{26}Cd_2N_6O_{10}S_2$ (MW = 919.52): C, 39.19; H, 2.85; N, 9.14; S, 6.97%. UV (H_2O): 330 nm (ε = 36905 dm^3 cm^{-1} mol^{-1}), 319 (39234), 281 (29426); UV (C_2H_5OH): 328 nm (ε, undefined), 316, 281.

$[Zn^{II}(\mu_2\text{-}O,O'\text{-}SO_4)(terpy)]_2\cdot 2H_2O$, 2·$2H_2O$. A clear solution of terpy (24 mg, 0.103 mmol) in ethanol (95%, 4 mL) was mixed with a clear solution of $ZnSO_4\cdot 7H_2O$ (Merck, 30 mg, 0.104 mmol) in water (3 mL) (1 : 1, terpy : Zn molar ratio). The mixture was heated at 353 K for 10 min and then stored at 293 K. Single crystals suitable for X-ray diffraction analysis formed after 4 days. The crystals were filtered off, washed twice with cold water, twice with a few drops of ethanol and then stored at 278 K. Yield, 50%. Anal. Found: C, 43.01; H, 2.86; N, 9.73. Calc. for $C_{30}H_{26}Zn_2N_6O_{10}S_2$ (MW = 825.42): C, 43.65; H, 3.17; N, 10.18%. UV (H_2O): 331 nm (ε = 36044 dm^3 cm^{-1} mol^{-1}), 319 (35824), 281 (29496); UV (C_2H_5OH): 329 nm (ε, undefined), 318, 281.

X-Ray crystallography

Data collection. Pale yellow prisms of **1**·$2H_2O$ (dimensions 0.20 × 0.15 × 0.10 mm) and **2**·$2H_2O$ (dimensions 0.30 × 0.20 × 0.10 mm) were selected at the polarising microscope and mounted on a glass fibre. The diffraction data were collected through a four-circle automatic Siemens P4 diffractometer, by using graphite-monochromatised Mo-Kα radiation (λ = 0.71073 Å). The accurate cell constants were determined *via* full-matrix least-squares refinement of the values of 29 carefully centred randomly selected reflections in the range $10 \le 2\theta \le 45°$ (Table 1). The data were collected at 293 ± 2 K, corrected for Lorentz-polarisation, and then for the absorption effects (ψ-scan technique). The independent observed reflections ($I > 2\sigma(I)$) were 2545 out of a total of 3082 collected reflections (R_{int} = 0.0084) for **1**·$2H_2O$ and 2284 out of a total of 2587 collected reflections (R_{int} = 0.0188) for **2**·$2H_2O$. Both structures crystallise in the triclinic space group $P\bar{1}$. Three standard reflections were monitored periodically (every 97 reflections) during the data collection, no appreciable decay was observed.

Structure solution and refinement. The structures were solved through the Patterson and Fourier techniques which allowed to locate all the atoms. All the non-hydrogen atoms were treated as anisotropic during the subsequent eight cycles of least-squares refinement. The hydrogen atoms from terpy were located in computed positions and left to ride on the atoms to which they are linked. The H-atoms for the co-crystallised water molecule were located from the Fourier-difference map and fully refined. All the H-atoms were treated as isotropic in the refinement cycles. For the structure of **2**·$2H_2O$ the extinction coefficient was refined and converged to 0.010(1). The agreement factors converged to $R1 = 0.0182$ and $wR2 = 0.0441$ for **1**·$2H_2O$ and $R1 = 0.0302$ and $wR2 = 0.0733$ for **2**·$2H_2O$ for the independent observed reflections with $I > 2\sigma(I)$. All the calculations were carried out using SHELXS97,[6] SHELXL97,[7] PARST97,[8] and ORTEP32[9] computer programs contained in the WinGX package[10] implemented on Pentium IV machines.

CCDC reference numbers 205815 and 205816.

See http://www.rsc.org/suppdata/dt/b3/b302779a/ for crystallographic data in CIF or other electronic format.

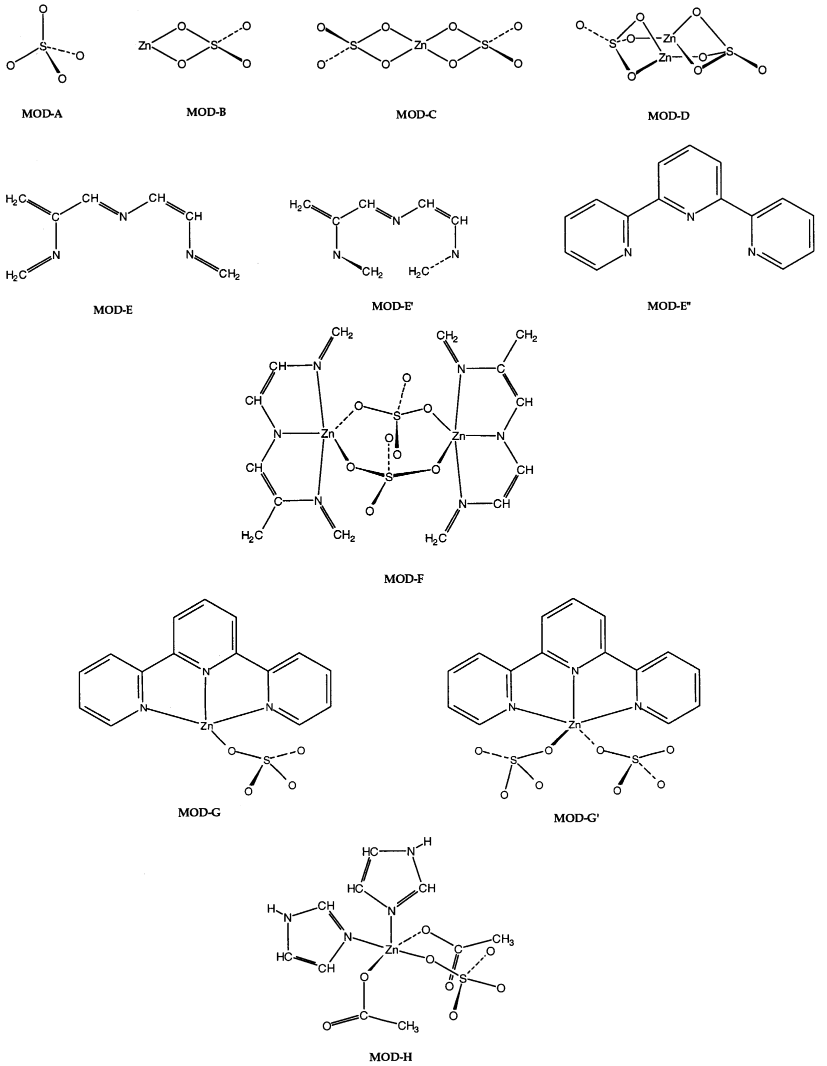

Scheme 3 Molecular models used for the semi-empirical quantum mechanics calculations (and in part for the density functional calculations). Overall charges are omitted for clarity purposes.

Spectroscopy

Solid state infrared spectra from a KBr matrix were obtained using a Perkin-Elmer FTIR 1600 spectrometer. The UV spectra were recorded by using a Perkin-Elmer EZ-201 spectrophotometer (operating at 20 °C).

Molecular modelling

Semi-empirical molecular orbital calculations. All the calculations were performed using the HyperChem 5.1 package.[11] The molecular structure for SO_4^{2-} (MOD-A) was optimised in the gas phase at several levels of approximation (ZINDO/1, MNDO, MNDO/d, PM3 and AM1).[12] The best results in terms of computed bond distances (when compared to experimental) were obtained through the AM1 level. Therefore the subsequent calculations were performed at the AM1 level for all the molecules. The other fully optimised molecules (Scheme 3) were $[Zn(O,O'\text{-}SO_4)]$ (MOD-B), $[Be(O,O'\text{-}SO_4)]$ (MOD-B′), $[Zn(O,O'\text{-}SO_4)_2]^{2-}$ (MOD-C), $[Be(O,O'\text{-}SO_4)_2]^{2-}$ (MOD-C″″), $[Zn(\mu_2\text{-}O,O'\text{-}SO_4)_2Zn]$ (MOD-D), $CH_2{=}N{-}C({=}CH_2){-}CH{=}N{-}CH{=}CH{-}N({=}CH_2)$ (MOD-E) and (MOD-E′) (as a model for terpy), terpy (MOD-E″), $[(\text{MOD-E})Zn(\mu_2\text{-}O,O'\text{-}SO_4)_2Zn(\text{MOD-E})]$ (MOD-F), $[(\text{MOD-E}'')Zn(O\text{-}SO_4)]$ (MOD-G), $[(\text{MOD-E}'')Zn(O\text{-}SO_4)_2]^{2-}$ (MOD-G′), $[Zn(Im)_2(O\text{-}OOCCH_3)_2(O\text{-}SO_4)]^{2-}$ (MOD-H), the adduct MOD-F ··· Be^{2+}, MOD-FBe, with the Be^{2+} cation at centre of cavity, and MOD-HW with MOD-H inside of a box 12 × 12 × 18 Å filled with 86 water molecules. The starting structure for MOD-F was based on the X-ray structure of **2**; whereas the starting structure for MOD-H was based on the X-ray structure of ATP-sulfurylase,[1a] and the starting structure for MOD-FBe was the optimised MOD-F molecule to which the guest cation was added *via* the graphical tools implemented in HyperChem.[11] The geometrical parameters for all the models were freely refined without any restraints, except for MOD-E, and the (MOD-E)Zn moiety of MOD-F and MOD-FBe whose atoms were restrained to planarity, and MOD-G, MOD-G′ and MOD-H whose Zn–N bond distances were restrained as reported below (Results and discussion). All the molecules were refined up to a RMS gradient of 0.04 kJ $Å^{-1}$ except for MOD-HW for which the final RMS gradient was 1.60 kJ $Å^{-1}$ (407 cycles). The analysis of the vibration modes did not show any negative frequencies. The UV spectra were computed by using the ZINDO/S level on the structures previously fully optimised at AM1.

Density functional calculations. All the density functional calculations have been performed by using the GAUSSIAN98/RevA.7[13] package implemented on an Origin 3800 SG machine at CINECA (Inter-University Computing Center, Casalecchio di Reno, Bologna, Italy). Geometry optimisations, population analysis and vibration frequencies calculations have been obtained by using the Becke3LYP method[14] and the LANL2DZ[14] basis set for all the atoms, unless otherwise specified

Table 2 Selected bond lengths (Å) for $[Cd^{II}(\mu_2\text{-}O^2,O',O''\text{-}SO_4)(terpy)]_2\cdot 2H_2O$, **1**·$2H_2O$

Cd1–N1	2.362(2)	S1–O4	1.435(2)
Cd1–N1′	2.318(2)	N1–C2	1.353(3)
Cd1–N1″	2.364(2)	N1–C6	1.336(3)
Cd1–O2	2.330(2)	N1′–C2′	1.338(3)
Cd1–O3	2.555(2)	N1′–C6′	1.337(3)
Cd1–O1_2	2.397(2)	N1″–C2″	1.337(3)
Cd1–O3_2	2.497(2)	N1″–C6″	1.342(3)
S1–O1	1.463(2)	O1–Cd1_2	2.397(2)
S1–O2	1.484(2)	O3–Cd1_2	2.497(2)
S1–O3	1.496(2)	Cd1 ··· Cd1_2	4.028(1)

Symmetry transformations used to generate equivalent atoms: _2: $-x + 1, -y + 1, -z + 1$.

(see below). The models analysed were: MOD-A (see above), MOD-C, $[Cd(O,O'\text{-}SO_4)_2]^{2-}$ (MOD-C′) and $[Ca(O,O'\text{-}SO_4)_2]^{2-}$ (MOD-C″), $[Mg(O,O'\text{-}SO_4)_2]^{2-}$ (MOD-C‴).

The molecules MOD-A through MOD-C‴ were analysed by using the 6-31G** basis set for the soft S atoms, whereas the metal and oxygen atoms were treated by using the LANL2DZ and 6-31G basis set,[14] respectively. The solvent effects were not taken into account for all the molecules. The geometrical parameters have been fully optimised without any restraints. The optimisation of the geometry was carried out up to the criteria implemented in GAUSSIAN98 (for maximum force and RMS force shifts, 0.000450, 0.000300 Hartrees/Bohrs, respectively; and for maximum displacement and RMS displacement 0.001800, 0.001200 Å, respectively). The analysis for the vibration frequencies was carried out for all the optimised molecules. No imaginary frequencies were computed. Molecular drawings for the optimised models were obtained through ORTEP32 package[9] (see above, X-ray diffraction).

Results and discussion

X-Ray crystallography

$[Cd^{II}(\mu_2\text{-}O^2,O',O''\text{-}SO_4)(terpy)]_2\cdot 2H_2O$, 1·$2H_2O$. The neutral binuclear complex particle contains two three-coordinate terpy molecules, two three-coordinate sulfato anions and two hepta-coordinate Cd(II) centres (Fig. 1, Tables 2 and 3). The structure is centrosymmetric, the inversion centre being inside the cavity built up by two metal ions, six oxygen atoms and two sulfur atoms. The asymmetric unit consists of a cadmium centre, a terpy molecule, a sulfato anion, and a co-crystallised water molecule. The metal ion is linked to the three nitrogen atoms from terpy and to four oxygen atoms, two of which are from a sulfato anion and the other two from the symmetry related anion. The sulfato anion has therefore three oxygen donors to the metal centres, whereas the fourth oxygen atom acts as an H-bond acceptor from the co-crystallised water molecule. The sulfato anion bridges two metal centres through the formation of two four-membered chelate rings; one of the oxygen atoms (namely O3) being linked to the two metal ions. This coordination mode for sulfato ligand has not been reported before. The metal ion coordinates to the N1, N1′, N1″, O2, O1_2 (_2: $-x + 1, -y + 1, -z + 1$) atoms in a distorted trigonal bipyramid arrangement; the N1 and N1″ atoms occupy the apical positions and N1′, O2, O1_2 the equatorial sites. Two additional longer bonds involve the bridging O3 and O3_2 atoms. The Cd–N bond lengths (2.362(2), 2.318(2) and 2.364 (2) Å for N1, N1′ and N1″, respectively, are in agreement with the values previously reported for $[Cd^{II}(terpy)Cl_2]$[15] and other similar Cd(II)-complexes with bipy (2,2′-bipyridine)[16] and phen (1,10-phenanthroline).[17] The Cd–O bond distances with the oxygen atoms from a sulfato are 2.330(2) (O2) and 2.555(2) (O3) Å, whereas those with the oxygen atom from the symmetry related sulfato are 2.397(2) (O1_2) and 2.497(2) (O3_2) Å. The bond angles at metal which involve the oxygen atoms only, are in the range 57.62(7) (O1_2–Cd1–O3_2) to 140.01(6)° (O1_2–Cd1–O2), the small values releating to the four-membered chelate rings. It should be noted that thiosulfato anion in $[(Me_2\text{-phen})Cd(\mu_2\text{-}S,S,O\text{-}S_2O_3)_2Cd(Me_2\text{-phen})]$ (Me_2-phen = 2,9-Me_2-1,10-phenanthroline),[18a] chelates a metal centre *via* S and O, the S atom being linked to the two Cd centres of the dimer. On the other hand, the structure of $[(Me_2\text{-phen})Ni(\mu_2\text{-}O^2,O',S\text{-}S_2O_3)_2\text{-}Ni(Me_2\text{-phen})]$ has the thiosulfato coordinated in a $\mu_2\text{-}O^2,O',S\text{-}S_2O_3$ mode.[18b]

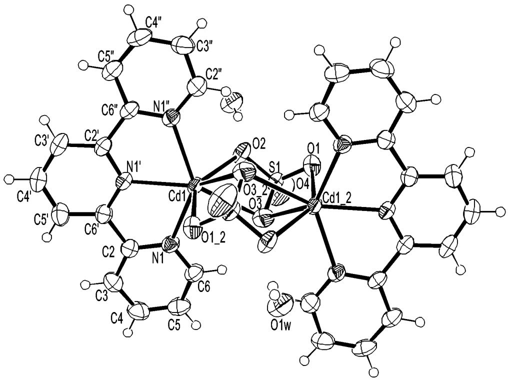

Fig. 1 Drawing of $[Cd^{II}(\mu_2\text{-}O^2,O',O''\text{-}SO_4)(terpy)]_2\cdot 2H_2O$, **1**·$H_2O$. The ellipsoids enclose 50% probability.

Table 3 Selected bond angles (°) for $[Cd^{II}(\mu_2\text{-}O^2,O',O''\text{-}SO_4)(terpy)]_2\cdot 2H_2O$, **1**·$2H_2O$

N1′–Cd1–O2	123.72(7)	N1″–Cd1–O3	136.05(7)
N1′–Cd1–N1	69.96(7)	O1_2–Cd1–O3	90.85(7)
O2–Cd1–N1	109.84(7)	O4–S1–O1	112.44(14)
N1′–Cd1–N1″	69.32(7)	O4–S1–O2	110.07(12)
O2–Cd1–N1″	85.03(7)	O1–S1–O2	110.60(12)
N1–Cd1–N1″	138.05(7)	O4–S1–O3	112.02(15)
N1′–Cd1–O1_2	95.97(7)	O1–S1–O3	105.74(12)
O2–Cd1–O1_2	140.01(6)	O2–S1–O3	105.70(11)
N1–Cd1–O1_2	86.60(7)	C6–N1–Cd1	124.49(17)
N1″–Cd1–O1_2	107.17(7)	C2–N1–Cd1	117.01(16)
N1′–Cd1–O3_2	133.44(7)	C6′–N1′–Cd1	118.89(15)
O2–Cd1–O3_2	87.88(7)	C2′–N1′–Cd1	120.05(16)
N1–Cd1–O3_2	135.31(7)	C2″–N1″–Cd1	122.91(17)
N1″–Cd1–O3_2	82.19(7)	S1–O1–Cd1_2	100.35(10)
O1_2–Cd1–O3_2	57.62(7)	S1–O2–Cd1	103.07(10)
N1′–Cd1–O3	149.80(7)	S1–O3–Cd1_2	95.17(10)
O2–Cd1–O3	57.98(6)	S1–O3–Cd1	93.21(9)
N1–Cd1–O3	81.17(7)	Cd1_2–O3–Cd1	105.75(8)

Symmetry transformations used to generate equivalent atoms: _2: $-x + 1, -y + 1, -z + 1$.

The metal centre for **1** deviates by 0.3054(2) Å from the plane defined by the three nitrogen atoms from terpy and by 0.0712(3) Å from the plane defined by O1_2, O2, N1′. Bond distances and angles within terpy are normal the dihedral angles between the three pyridyl systems being 5.7 (rings 1/2), 10.0 (1/3) and 4.9° (2/3). The S1–O4 bond length is 1.435(2) Å, whereas different lengthening effects are observed for S–O bonds relevant to the oxygen donors. The largest distance is found for S1–O3, 1.496(2) Å (O3 bridges two metal centres). As expected the two chelating SO_2-groupings have the narrowest O–S–O bond angles (105.7(1)°).

The co-crystallised water molecule (O1W) acts as a hydrogen bond donor to O4 (O ··· O, 2.848(3) Å; O ··· H–O 165(1)°) and to O2_2 (2.847(3) Å; 167(1)°). O1W is also a hydrogen bond acceptor from C5 (O ··· C, 3.316(3) Å; O ··· H–C 170(1)°) and C3′ (3.361(3) Å; 121(1)°). The terpy systems from different molecules are piled parallel each other, and the contact distances are as short as 3.363(3) Å, so that the crystal is stabilised by extensive staking interactions between the π-systems (Fig. 2).

Table 4 Selected bond lengths (Å) for $[Zn^{II}(\mu_2\text{-}O,O'\text{-}SO_4)(terpy)]_2\cdot 2H_2O$, **2**·$2H_2O$

Zn1–N1	2.207(2)	S1–O4	1.441(2)
Zn1–N1′	2.080(2)	N1–C2	1.344(4)
Zn1–N1″	2.163(2)	N1′–C2′	1.336(4)
Zn1–O3	1.956(2)	N1″–C2″	1.343(4)
Zn1–O2_2	1.975(2)	N1″–C6″	1.347(4)
S1–O1	1.432(2)	O2–Zn1_2	1.975(2)
S1–O3	1.495(2)	Zn1 ··· Zn1_2	4.148(1)

Symmetry transformations used to generate equivalent atoms: _2: $-x + 2$; $-y + 1$; $-z + 1$.

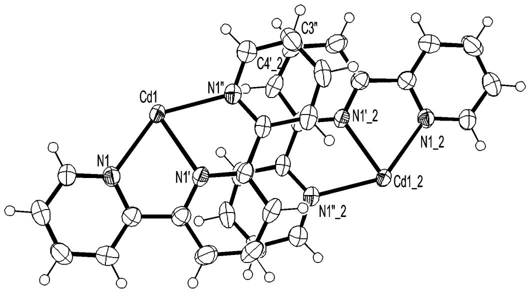

Fig. 2 Stacking interactions which involve the terpy moieties for **1**·$2H_2O$. The view is almost perpendicular to the mean plane of the pyridyl rings.

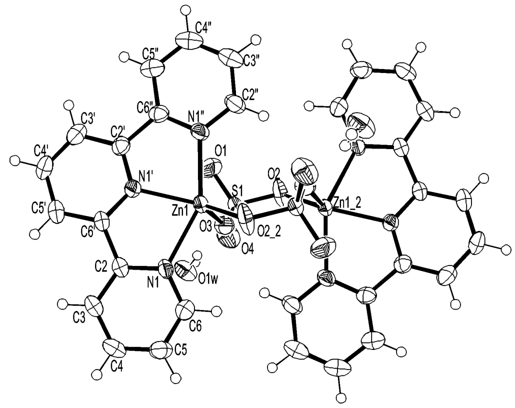

Fig. 3 Drawing of $[Zn^{II}(\mu_2\text{-}O,O'\text{–}SO_4)(terpy)]_2\cdot 2H_2O$, **2**·$2H_2O$. The ellipsoids enclose 50% probability.

Table 5 Selected bond angles (°) for $[Zn^{II}(\mu_2\text{-}O,O'\text{-}SO_4)(terpy)]_2\cdot 2H_2O$, **2**·$2H_2O$

O3–Zn1–O2_2	107.32(10)	O4–S1–O2	108.77(15)
O3–Zn1–N1′	115.42(9)	O1–S1–O3	110.37(14)
O2_2–Zn1–N1′	134.70(10)	O4–S1–O3	107.54(14)
O3–Zn1–N1″	107.66(9)	O2–S1–O3	107.46(13)
O2_2–Zn1–N1″	104.83(11)	S1–O3–Zn1	135.48(13)
N1′–Zn1–N1″	76.45(9)	C2′–N1′–Zn1	118.33(18)
O3–Zn1–N1	91.87(9)	C6′–N1″–Zn1	120.57(19)
O2_2–Zn1–N1	90.30(10)	S1–O2–Zn1_2	128.16(14)
N1′–Zn1–N1	74.47(9)	C2–N1–Zn1	115.80(19)
N1″–Zn1–N1	149.88(9)	C6–N1–Zn1	126.22(19)
O1–S1–O4	112.56(17)	C2″–N1″–Zn1	127.3(2)
O1–S1–O2	109.97(15)	C6″–N1″–Zn1	114.38(19)

Symmetry transformations used to generate equivalent atoms: _2: $-x + 2$, $-y + 1$, $-z + 1$.

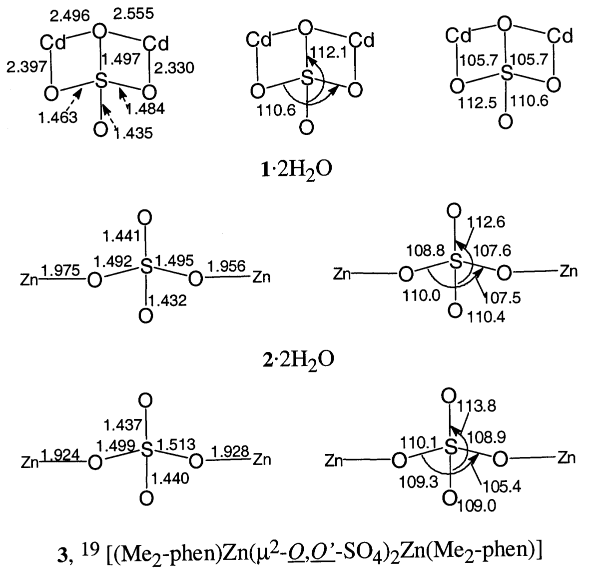

Scheme 4 Selected geometrical parameters (distances, Å; angles, °) around the sulfur atoms for **1**·$2H_2O$, **2**·$2H_2O$, and **3**.[19]

$[Zn^{II}(\mu_2\text{-}O,O'\text{-}SO_4)(terpy)]_2\cdot 2H_2O$, 2·$2H_2O$. The coordination sphere around the metal centre is pseudo-trigonal bipyramidal (Fig. 3, Tables 4 and 5) with the nitrogen atom (N1′) from the central pyridyl ring of terpy and two oxygen atoms (O3, O2_2) from two bridging sulfato groupings at the equatorial positions, and the two nitrogen atoms (N1, N1″) from the external pyridyl rings of terpy at the apical sites. The dimeric molecule has a crystallographic inversion centre midway the two metal ions. Interestingly, the two sulfato anions behave in a different fashion with respect to the same groupings of **1**. In fact, they bridge the metal centres through two distinct oxygen atoms, and no oxygen atoms are linked to two metal centres. Two oxygen atoms are terminal and not involved in significant bonding interactions to the Zn(II) ions. The Zn–N bond distances are 2.207(2), 2.163(2) and 2.080(2) Å (central). The Zn–O bond distances are 1.975(2) (O2_2) and 1.956(2) Å (O3), significantly longer than those found for $[(Me_2\text{-phen})Zn(\mu_2\text{-}O,O'\text{-}SO_4)_2Zn(Me_2\text{-phen})]$,[19] **3**, that contains two pseudo-tetrahedral zinc cations and a coordination ring similar to that for **2**. The selected geometrical parameters for the sulfato ligands for **1**, **2** and **3** are reported in Scheme 4. It is evident that the S–O(t) (t, terminal) and S–O(d) (d, donor) bond distances are close for the three complex molecules and lie in the range 1.43–1.45 and 1.46–1.51 Å, respectively. The formation of two four-membered chelate rings for **1** leads to a larger strain around the sulfur atom, as shown by the O–S–O bond angles which are in the range 105.7–112.5°, whereas those for **2** are closer to the idealised values of 109.5°.

The elongated cavities of the $Zn(\mu_2\text{-}O,O'\text{-}SO_4)_2Zn$ system for **2**, align approximately along the crystallographic *b* axis in the crystal structures (Fig. 4). The average inter-cluster distance is about 9.767 Å, which is the crystallographic repeat of the *b* axis. The distance between two symmetry related O3 atoms (roughly the diameter of the cavity) is 3.245 Å. By taking into account the van der Waals radius for oxygen (1.5 Å),[20] a narrowest cavity diameter of 0.245 Å is estimated for **2**. It should be noted that the entrances of the cavity are hindered by C2–H and C6″–H groupings from the pyridyl rings. As a consequence the cavity is too small to host a water molecule. In fact, the co-crystallised water molecule is external to the cavity. This analysis suggested modelling investigations to shed light on the cavity conformation (see below, semi-empirical molecular orbital methods) in the gas phase. The complex molecules **2** are piled in a way that the terpy moieties are almost perpendicular to a line which connects the vertices of the cell at $x = 0$, $y = 0$, $z = 1$, and $x = 1$, $y = 1$, $z = 0$. Inter-atomic contact distances between parallel terpy systems as short as 3.319 Å show the presence of strong inter-molecular stacking interactions between the dimers.

The co-crystallised water molecule O1W is the hydrogen donor to the terminal O4 atom (O ··· O, 2.835 Å; O–H ··· O, 160°) and to the metal-bound O2 atom ($-x + 2$, $-y + 1$, $-z$) (O ··· O, 2.953 Å; O–H ··· O, 169°).

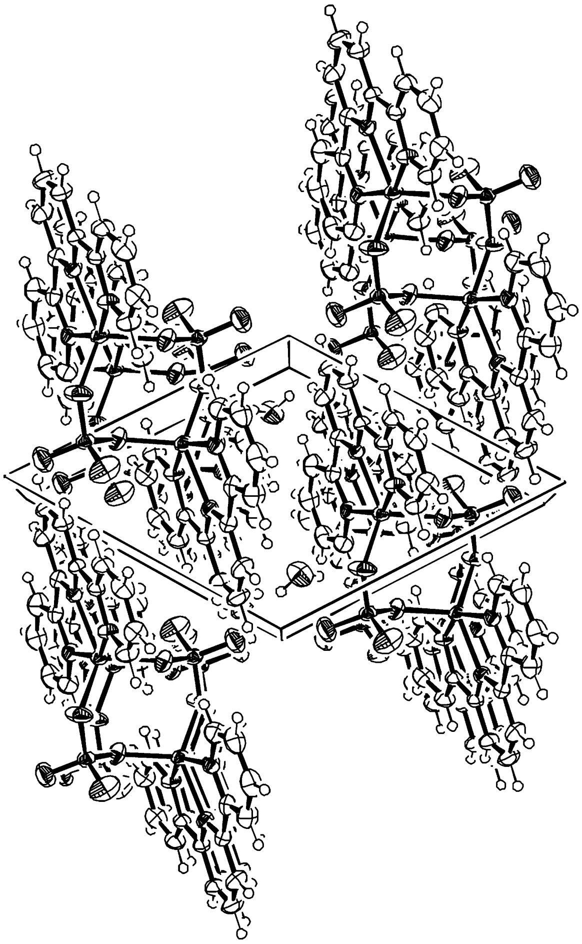

Fig. 4 Cavities for **2**·2H$_2$O as viewed approximately along the crystallographic *b* axis.

Infrared data

Selected absorption bands are at 1112 (strong and broad) and 618 (medium) cm^{-1} for **1**·2H$_2$O, and 1122 (strong and sharp) and 614 (medium) for **2**·2H$_2$O (Table 6). The spectrum of free sulfate (the molecule belongs to the T_d point group) consists of two absorption bands at *ca.* 1140 cm^{-1} ($\nu_3°$ stretching mode, ν_{asym}) and at *ca.* 614 cm^{-1} ($\nu_4°$ bending mode, δ_{asym}).[21] The coordination of sulfate to cations decreases the symmetry of the group and the $\nu_3°$ and $\nu_4°$ modes are split. Furthermore, the infrared-inactive $\nu_2°$ bending mode (free sulfate) gives an active mode, and the Raman-active $\nu_1°$ mode (ν_{symm}) is made infrared-active once the symmetry is lowered. In the case the SO$_4$-site symmetry is lowered from T_d to C_{2v} as happens for orthorhombic MgSO$_4$, triplets centred at 1166 cm^{-1} (ν_3 modes) and 624 cm^{-1} (ν_4 modes) are found.[21] The structure of **2** has C_{2v} symmetry at sulfato and the strong band at 1122 cm^{-1} is therefore attributable to a ν_3 mode. The other two ν_3 modes are tentatively assigned to the bands at 1225 and 1038 cm^{-1}. The bands at 657, 614 and *ca.* 590 cm^{-1} (shoulder) are attributed to the ν_4 modes. The symmetry of the sulfato groups in **1** is C_1. As a consequence the absorption bands at 1112 cm^{-1} (ν_3 modes) and 618 cm^{-1} (ν_4 modes) are broad as they consist of several effects close each other.

Table 6 Selected infrared frequencies (cm^{-1}, intensity in parentheses, km mol^{-1}) for the sulfato-complexes as computed through Hessian analysis applied to the structure-optimised molecules at the Becke3LYP (LANL2DZ; 6-31G**, S) level as well as through AM1 semi-empirical molecular orbital methods. The experimental frequencies as obtained at the solid state (KBr pellets) are also reported for comparative purposes

	Vibration		
Molecule	ν_3	ν_3	ν_4
AM1			
MOD-B	1197 [131.16]	1010 [212.74]	643 [162.76]
MOD-C	1045 [181.03]	954 [535.10]	490 [84.22]
MOD-D	1140 [397.88]	835 [479.05]	692 [324.42]
MOD-F	1096 [325.64]	914 [224.54]	589 [121.34]
MOD-G	1105 [172.01]	1046 [225.43]	610 [128.64]
MOD-G′	1019 [320.85]	978 [318.77]	590 [95.45]
MOD-H	1031 [181.16]	983 [155.79]	586 [97.41]
DFT			
$[Mg(O,O'\text{-}SO_4)_2]^{2-}$	1208 [338.99]	1109 [824.84]	642 [15.54]
$[Ca(O,O'\text{-}SO_4)_2]^{2-}$	1191 [341.83]	1099 [874.34]	603 [145.15]
$[Zn(O,O'\text{-}SO_4)_2]^{2-}$	1205 [324.75]	1101 [911.12]	623 [197.61]
$[Cd(O,O'\text{-}SO_4)_2]^{2-}$	1196 [317.00]	1092 [970.83]	606 [155.81]
Experimental			
1·2H$_2$O	1112 [strong, broad]	—	618 [medium]
2·2H$_2$O	1122 [strong]	1038 [medium]	614 [medium]

Molecular modelling

Semi-empirical molecular orbital calculations. *Structures.* The computed S–O bond distance at the AM1 level for free sulfate anion (MOD-A) is 1.463 Å (found for uronium sulfate, 1.466–1.483 Å).[22] The computed S–O(d) bond distances for [Zn(*O*,*O*′-SO$_4$)] (MOD-B, Fig. 5) are 1.642 Å, whereas the computed S–O(t) and Zn–O distances are 1.370 and 1.958 Å, and the O(d)–S–O(d) angle is 85.6°. On adding a second sulfato chelating ligand to MOD-B to form pseudo-tetrahedral [Zn(*O*,*O*′-SO$_4$)$_2$]$^{2-}$ (MOD-C), the computed S–O(d) distances decrease to 1.549 Å whereas the S–O(t) lengths increase to 1.410 Å.

The optimised structure of [Zn(μ$_2$-*O*,*O*′-SO$_4$)$_2$Zn] (MOD-D) has S–O(d) bond distances (1.522, 1536 Å) shorter than the corresponding ones for MOD-C. It should be noted that each sulfato ligand behaves as a chelate towards one metal centre and as monodentate towards a second one. The metal centres are therefore three-coordinate. This coordination arrangement for sulfato corresponds to mode **IV** (Scheme 2). Only two structures that show this mode, to our knowledge, have been reported so far; the pseudo-octahedral complex [Ru^{III}(μ$_2$-*O*,*O*′,*O*″-SO$_4$)(*S*,*S*′-(^{i}Pr$_2$-thiophosphoryl)amide-1)-(PPh$_3$)]$_2$[23] for which the S–O(d) (chel) and S–O(d) bond distances are 1.499 and 1.527, and 1.462 Å, and the pseudo-octahedral complex [Ru^{II}(μ$_2$-*O*,*O*′,*O*″-SO$_4$)(PPh$_3$)$_2$(*S*-SO$_2$)]$_2$[24] for which the S–O(d) (chel) and S–O(d) bond distances are 1.498 and 1.489, and 1.469 Å. The O(d)–S–O(d) bond angles are 101.9° for both the structures when the chelating ring is considered, whereas values in the range 109.2–110.8° have been found for the other O(d)–S–O(d) angles. Therefore, MOD-D reproduces well the trend of the experimental geometrical parameters of the coordination ring even though the metal considered for the computation is three-coordinate Zn(II) instead of octahedral Ru(II,III). These findings encouraged us to compute other binuclear metal-sulfato complexes.

MOD-E was optimised as a model for the terpy ligand in the planar *cis*,*cis* conformation; it allows the optimisation of ternary complex molecules at a low computational cost, when compared to terpy. The computed intramolecular N ··· N contact distances for free MOD-E are *ca.* 5% (or less) larger than the corresponding ones for optimised terpy (MOD-E″).

The computed S–O(d) bond distances for [(MOD-E)-Zn(μ$_2$-*O*,*O*′-SO$_4$)$_2$Zn(MOD-E)] (MOD-F) are 1.510 Å, in perfect agreement with the values found in the solid state for **2** (1.495 Å). The computed S–O(t) bond distances are 1.384 and 1.415 Å which compare well with the experimental values at the

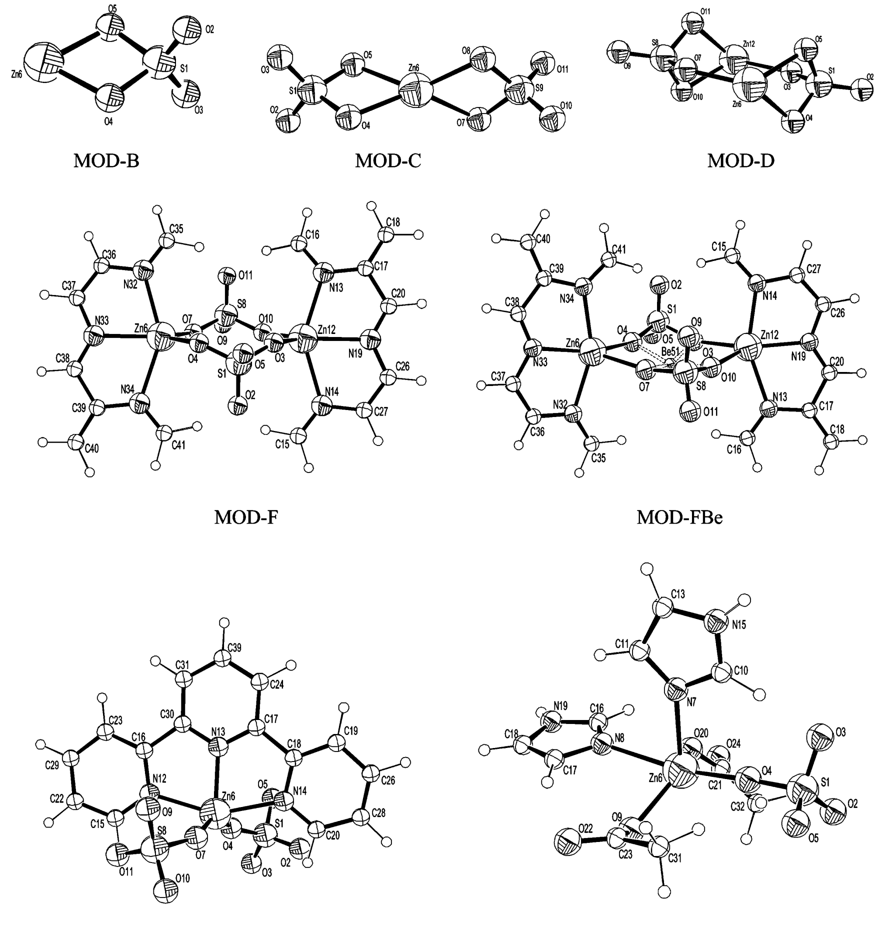

MOD-B MOD-C MOD-D

MOD-F MOD-FBe

MOD-G’ MOD-H

Fig. 5 ORTEP drawings of the selected optimised structures through the semi-empirical molecular orbital AM1 method or through the hybrid density functional DFT-Becke3LYP/(LANL2DZ; S, 6–31G**) method. The atom numbering is that used in the Tables of geometrical parameters reported in the ESI.† Further model structures are also reported in the ESI.

solid state (1.436 Å, average). The computed Zn–O(d) is 2.026 Å (found 1.975 and 1.956 Å). Even the computed bond angles around the sulfur atoms (O(d)–S–O(d), 105.8°; O(t)–S–O(t), 116.9°; O(d)–S–O(t), 106.9–109.8° (range)) compare well with experiment: 107.5°; 112.6°; 107.6–110.4° (average). In conclusion, this level of theory represents adequately the sulfato ligand in this type of bi-nuclear complexes.

The cavity size for MOD-F is significantly larger than that for **2**. In fact the shortest distance between two opposite O(d) atoms is 4.077 Å in MOD-F and 3.245 Å in **2**. This means that the distances between the two van der Waals surfaces is *ca.* 1.08 Å. We thought that such a cavity could host small cations such as Be^{2+}, Al^{3+} or even Li^{+} (ionic radii 0.31, 0.50, 0.60 Å).[25] For this reason the models MOD-FBe, MOD-FAl, MOD-FLi were built and submitted to optimisation. Interestingly, MOD-FBe converged, with the alkaline-earth cation almost at the centre of the cavity. The Zn ··· Zn intramolecular contact distances increased to 5.500 Å, whereas the S–O(d) and S–O(t) bond distances converged to 1.637 and 1.361 Å, respectively, upon adduct formation. MOD-FAl and MOD-FLi did not converge.

The coordination arrangements for [(terpy)Zn(*O*-SO_4)] (MOD-G) and $[(\text{terpy})\text{Zn}(O\text{-SO}_4)_2]^{2-}$ (MOD-G′) are pseudo-square-planar and pseudo-trigonal bipyramidal, respectively. The two sulfato ligands and the central nitrogen atom of MOD-G′ occupy two equatorial positions (restraints: Zn–N (middle) and Zn–N (peripheral), 2.08 and 2.18 Å). The S–O(t) bond distances for MOD-G′ converged to the range 1.417–1.438 Å, whereas the Zn–O bond distance converged to 2.017 Å.

The fully optimised structure of MOD-H has a pseudo-trigonal pyramidal coordination arrangement (see Fig. 5). Two oxygen atoms from distinct carboxylato ligands (monodentate) and the nitrogen atom of an imidazole ligand occupy the equatorial positions, an oxygen atom from sulfato and a nitrogen atom from the second Im occupy the axial positions. The freely refined Zn–O(S) bond distance is 2.016 Å, whereas the Zn–O-(C) bond distances are 2.157 and 2.163 Å. Both of the acetates are monodentate towards the metal. The C–O(d) bond distances are 1.302 Å, whereas the C–O(t) bond distances are 1.261 Å.

The aggregate MOD-HW has an overall structure close to that of MOD-H. The Zn–O(S), S–O(d) and S–O(t) bond distances are 2.105, 1.466 and 1.434 Å, respectively. Most of the water molecules cluster around the sulfato ligand causing a lengthening effect on the Zn–O(S) distance.

Spectroscopy. The computed infrared spectra for selected models are briefly reported and commented especially for the vibrations relevant to the sulfato ligand (see Table 6). The spectrum for MOD-F has selected frequencies at 1096 (325.64 km mol^{-1}, ν_3(asym) SO_2(t)) and 914 cm^{-1} (224.54). The motion ν(asym) SO_2(d) has frequency 826 cm^{-1} (779.91), whereas the vibration ν(sym) SO_2(d) has frequency 816 cm^{-1} (357.83). A ν_4(bending) for sulfato occurs at 589 cm^{-1} (121.34). The values compare well with the data reported above for **2**·H_2O and are red-shifted by just 20 cm^{-1} with respect to experiment.

The computed spectra for MOD-G and MOD-G′ have selected frequencies at 1105 (172.01) and 1019 cm^{-1} (320.85), ν_3(asym) SO_3(t), at 1046 (225.43) and 978 cm^{-1} (318.77), ν_3(asym) SO_3(t) combined with motions on terpy, at 610 (128.64) and 590 cm^{-1} (95.45), at 559 (44.15) and 530 cm^{-1} (102.09), both mostly ν_4(bending) sulfato. The frequencies compare well with the corresponding ones for MOD-F, and help assigning the spectra of monodentate-sulfato derivatives. The computed infrared spectrum for MOD-FBe has selected effects at 1249 (107.01, stretching SO(t)) and 585 cm^{-1} (116.81, bending SO_4), showing that the adduct formation has a significant blue shift for the stretching motion.

The computed spectrum for MOD-H has selected frequencies relevant to the ν_3 stretching modes at 1031 (181.16, combined with some CH_3-bending), 983 (155.79) and 949 cm^{-1} (115.00). The ν_4 bending modes occur at 586 (97.41) (see ESI†), and at 520 cm^{-1} (76.40). Other vibrations are at 1680 (261.94, ν C–O(d)) and 1951 cm^{-1} (467.12, ν C=O(t)). The frequencies relevant to sulfato are very close to the corresponding ones for MOD-G and MOD-G′ and this shows that terpy–metal–sulfato systems should vibrate similarly to the metal sites in sulfurylase.

The computed UV spectrum of MOD-D has only a weak absorption at 230 nm (0.042 oscillator strength) and is due to transition #12 between MO #30 (mostly O(t) atomic orbitals with a small contribution of O(d) aos) and MO #33 (LUMO, mostly zinc aos with small contributions from oxygen aos). This means that the $ZnSO_4$ grouping is a poor chromophore in the ultraviolet region. The computed spectrum for MOD-F has an intense absorption at 302 nm (1.974) (due to transition #6 between MO #82 and MO #85). The datum compares well with the absorptions at 331 and 319 nm in the spectrum of **2**·2H$_2$O. The computed UV spectrum for MOD-G and MOD-G′ has an intense band at 329 nm (0.779). The computed UV spectrum of MOD-H has effects at 249 (0.233, transition #15, from MO #60 mostly Im and carboxylato aos to MO #67, LUMO, pure Im aos) and 233 (0.217 transition #23, MO #58, contribution from Im aos carboxylato aos and smaller contribution from sulfato aos, to MO #68, pure Im aos). Therefore UV spectroscopy for L–metal–sulfato systems is dominated by the transitions relevant to the π-conjugate groupings present in the L ligand.

Heat of formation and the MOD-FBe adduct. The conformations of the Zn(SO$_4$)$_2$ moiety for MOD-F and MOD-G are very similar to each other but different from that of **2**. A model structure, namely MOD-G″, with the torsion angles for the Zn(*O*-SO$_4$)$_2$ grouping equal to that of **2** was built by starting from MOD-G′. The computed heat of formation for MOD-G′ and MOD-G″ is −771.7485 (see ESI†) and −732.2272 kJ, respectively. Even though the difference (*ca.* 37.6560 kJ) is a low limit estimation for the energy required to change the conformation of the coordination ring for **2**, it suggests that the rearrangement can be reached through heating, or linking interactions between the cavity atoms and an approaching small positive cation. In fact the beryllium adduct was regularly optimised. The heat of formation reaction of the MOD-FBe adduct from MOD-F and Be^{2+} is −1344.8011 kJ.

Density functional computations. The computed S–O bond distances for free sulfate as obtained by using the (6-31G**, S,O) basis set (BS1) are 1.526 Å (see also ref. 5*c*), and compare well with the experimental values in the solid state from accurately refined X-ray structures for not metal-bound sulfate anion.[26*a*,*b*] The lengthening effect of bond distances introduced by theory with respect to experiment, in the solid state was previously noted.[26*c*] In the case the (6-31G**, S; 6-31G, O) basis set (BS2) is used, the optimised S–O bond distance is 1.537 Å, elongated by just 0.7% (0.01 Å) with respect to the computations at BS1. This small effect suggested to perform the subsequent computations on the metal–sulfato species at BS2. The computed S–O(t) bond distances for the [M(*O*,*O*-SO$_4$)$_2$]$^{2-}$ (MOD-C, -C′, -C″, -C‴) molecules increase slightly in the order 1.493 (Mg), 1.493 (Zn), 1.496 (Cd), 1.498 Å (Ca), and show a significant shortening when compared to the computed values for free sulfate. The computed M–O(S) bond distances are 2.015 (Mg), 2.047 (Zn), 2.232 (Cd), 2.352 Å (Ca) and correlate well with the ionic radii (coordination number, cn, 4) for the divalent metal cations[25] (the value for Ca^{2+} has been estimated as 1.02 from the values from ref. 25 for cn 10 and 8). The computed O(d)–S–O(d) and O(t)–S–O(t) bond angles for MOD-C through MOD-C‴ are 97.9, 114.0° (Mg), 98.5, 114.0° (Zn), 100.6, 113.9° (Cd), 100.3, 113.8° (Ca), respectively. The results show that the metal ligation to sulfate changes the structural arrangement around sulfur, from pure tetrahedral (T_d) in free sulfate to C_{2v} symmetry for metal bound-sulfato. The magnitude of effects on structural parameters by Zn(II) is similar to that by Mg(II) and larger than those by Cd(II) and Ca(II). The search of published real structures that contains the M(*O*,*O*-SO$_4$)$_2$$^{2-}$ groupings gave seven results; the complexes contain Ho(III), Y(III), Tb(III), Dy(III), Er(III), Yb(III)[27] and Th(IV),[28] cations that are also linked to four water molecules, and four urea molecules. In the case of the Ho(III) derivative the S–O(d) and S–O(t) bond distances are 1.492 and 1.458 Å, respectively.

The energies for the formal complex formation reactions computed from the total electronic energies without any correction for the basis set superposition effect are −3293.2179 (Zn), −3155.1166 (Mg), −3083.8329 (Cd) and −2721.0075 kJ (Ca), respectively. The computed frequencies for the S–O stretching motions are in the ranges 1208–1109 (Mg), 1205.4–1100.7 (Zn), 1195.7–1091.9 (Cd), and 1190.7–1099.1 cm^{-1} (Ca). The values compare well with the corresponding ones at the AM1 level for MOD-C (Tables 6).

Conclusions

Novelty

The work produced a series of results on the coordinating properties of sulfate. The synthesis and crystal growth of two new metal–sulfato complexes unveiled an unprecedented arrangement for SO$_4$$^{2-}$ that forms a strong μ_2-*O*^{2},*O*′,*O*″ bridge between two Cd^{2+} cations by donating *via* three oxygen atoms and gives a compact Cd(SO$_4$)$_2$Cd cavity with a short Cd ··· Cd intra-dimer contact (4.028 Å). The distance between the two μ-O^2 oxygen atoms is 3.049 Å so that the two van der Waals spheres are almost in close contact. The close approach of the two SO$_4$$^{2-}$ anions is stabilised *via* two intra-dimer (N)C–H ··· O(S) hydrogen bonds (C ··· O, 3.079 Å) and is reflected in the high density of the crystals (1.943 g cm^{-3}). These data mean that compact small clusters of SO_4 or SO_4/PO_4 groups as stabilised by metal ions and suitable hydrogen bonds can be formed in living systems and may intervene in the efficient transport of sulfate and in the formation of mixed phospho-sulfate esters.

Cavity

Unexpectedly, in the case of the smaller zinc cation the coordination cavity is less compact than that for the larger cadmium derivative, and the density of crystals of **2** is 1.795 g cm^{-3}. Because of the coordination mode μ_2-*O*,*O*′-SO$_4$, the cavity for **2** is reasonably more flexible than that for **1** (even though still too narrow to accommodate small species, diameter of *ca.* 0.25 Å). However, the molecular modelling study showed that the cavity is flexible enough to host a Be^{2+} cation at the centre of the hole (MOD-F and MOD-FBe). This suggests a potential selective capturing ability by **2** and similar Zn(II)-complexes, towards Be^{2+} cations.

Biology

Metal–sulfato complexes acquire increasing interest because the importance of speciation studies related to toxic/essential metal ions in aqueous systems (such as drinking and other types of waters) or in living systems. The percentage of species of the type [M(*O*,*O*-SO$_4$)] and [M(*O*,*O*-SO$_4$)$_2$]$^{2-}$ could be relatively high in the case of large concentrations of sulfate anion. If the aqueous system contains heteroaromatic ligands such as imidazole or pyridine derivatives, binuclear complexes with bridging sulfato can be formed, as shown for Zn and Cd in this work or for Mn,[1*d*] Co,[28] and Cu[29] by other workers. The structural variability of sulfate shown through the coordination modes **I**–**VII** and the new mode **VIII** found for $\mathbf{1}\cdot 2H_2O$ is an interesting point as regards the so called "sulfate shift"[1d] (a term similar to "carboxylate shift" or "phosphate shift") which is related to the different bridging modes of biologically important groups,[31] that play subtle and important roles in a huge number of catalytic processes.

Finally, the experimental and theoretical analysis from this work shows that infrared spectroscopy and semi-empirical molecular orbital calculations at the AM1 level are low-cost and suitable tools to analyse metal–sulfato complexes and their adducts with enzymes.

Acknowledgements

The authors gratefully acknowledge Mr F. Berrettini (Centro Interdipartimentale di Analisi e Determinazioni Strutturali CIADS, University of Siena) for technical assistance in the X-ray data collection. The University of Siena are acknowledged for funding. Consorzio Interuniversitario per la Ricerca nella Chimica dei Metalli nei Sistemi Biologici (CIRCMSB, Bari) is acknowledged for grants to Gabriella Tamasi for the years 2002 and 2003.

References

1 (*a*) T. C. Ullrich, M. Blaesse and R. Huber, *EMBO J.*, 2001, **20**, 316; (*b*) C. S. Bond, P. R. Clements, S. J. Ashby, C. A. Collyer, S. J. Harrop, J. J. Hopwood and J. M. Guss, *Structure*, 1997, **5**, 277; (*c*) I. Boltes, H. Czapinska, A. Kahnert, R. Von Buelow, T. Dirks, B. Schmidt, K. Von Figura, M. A. Kertesz and I. Uson, *Structure*, 2001, **9**, 483; (*d*) C. He, V. Gomez, B. Spingler and S. J. Lippard, *Inorg. Chem.*, 2000, **39**, 4188; (*e*) D. Jamieson, *Nature (Genetics)*, 2002, **31**, 228; (*f*) G. Kampf, M. S Lüth, L. E. Kapinos, J. Müller, A. Holý, B. Lippert and H. Sigel, *Chem. Eur. J.*, 2001, **7**, 1899; (*g*) C. F. Moreno-Luque, R. Griesser, J. Ochocki and H. Sigel, *Z. Anorg. Allg. Chem.*, 2001, **627**, 1882; (*h*) B. Song, R. K. O. Sigel and H. Sigel, *Chem. Eur. J.*, 1997, **3**, 29.

2 (*a*) J. Moriyama, H. Nishiguchi, T. Ishihara and Y. Takita, *Ind. Eng. Chem. Res.*, 2002, **41**, 32; (*b*) S. N. Koyande, R. G. Jaiswal and R. V. Jayaram, *Ind. Eng. Chem. Res.*, 1998, **37**, 908.

3 (*a*) M. I. Khan, S. Cevik and R. J. Doedens, *Chem. Commun.*, 2001, 1930; (*b*) F. A. Cotton and R. A. Walton, *Multiple Bonds Between Metal Atoms*, Wiley, New York, 1982; (*c*) J. Reedijk, *Inorg. Chim. Acta*, 1992, **198–200**, 873.

4 The Cambridge Crystallographic Data Base, Version 5.24, November 2002.

5 (*a*) R. Cini and C. Pifferi, *J. Chem. Soc., Dalton Trans.*, 1999, 699; (*b*) R. Cini, D. Chindamo, M. Catenaccio, S. Lorenzini, E. Selvi, F. Nerucci, M. P. Picchi, G. Berti and R. Marcolongo, *Ann. Rheum. Dis.*, 2001, **60**, 962; (*c*) C. Pifferi, M. P. Picchi and R. Cini, *Polyhedron*, 2000, **19**, 69.

6 G. M. Sheldrick, SHELXS97, Program for the Solution of Crystal Structures, University of Göttingen, 1997.

7 G. M. Sheldrick, SHELXL97, Program for the Refinement of Crystal Structures, University of Göttingen, 1997.

8 M. Nardelli, PARST97, A System of Computer Routines for Calculating Molecular Parameters from Results of Crystal Structure Analyses, University of Parma, 1997.

9 C. K. Johnson and M. N. Burnett, ORTEP-3 for Windows, Oak Ridge National Laboratory. 32-bit Implementation by L. J. Farrugia, University of Glasgow, 1998.

10 L. J. Farrugia, WinGX an Integrated System of Windows Program s for the Solution, Refinement and Analysis of Single Crystal X-Ray Diffraction Data, Version 1.64.04, University of Glasgow, 1999.

11 HyperChem™, Molecular Modeling System, Release 5.1 Pro for Windows, Hypercube Inc., Gainesville, FL, 1997.

12 HyperChem™, Reference Manual, Hypercube Inc., Gainesville, FL, 1997.

13 M. J. Frisch, G. W. Trucks, H. B. Schlegel, G. E. Scuseria, M. A. Robb, J. R. Cheeseman, V. G. Zakrzewski, J. A. Jr. Montgomery, R. E. Stratmann, J. C. Burant, S. Dapprich, J. M. Millam, A. D. Daniels, K. N. Kudin, M. C. Strain, O. Farkas, J. Tomasi, V. Barone, M. Cossi, R. Cammi, B. Mennucci, C. Pomelli, C. Adamo, S. Clifford, J. Ochterski, G. A. Petersson, P. Y. Ayala, Q. Cui, K. Morokuma, D. K. Malick, A. D. Rabuck, K. Raghavachari, J. B. Foresman, J. Cioslowski, J. V. Ortiz, A. G. Baboul, B. B. Stefanov, G. Liu, A. Liashenko, P. Piskorz, I. Komaromi, R. Gomperts, R. L. Martin, D. J. Fox, T. Keith, M. A. Al-Laham, C. Y. Peng, A. Nanayakkara, C. Gonzalez, M. Challacombe, P. M. W. Gill, B. Johnson, W. Chen, M. W. Wong, J. L. Andres, C. Gonzalez, M. Head-Gordon, E. S. Replogle, J. A. Pople, *Gaussian 98, Revision A.7*, Gaussian, Inc., Pittsburgh PA, 1998.

14 A. Frish and M. J. Frisch, *Gaussian 98, User's Reference* (2nd Edition), Gaussian, Inc., Carnegie Office Park, Building 6, Pittsburgh, PA 15106.

15 J. Pickardt, B. Staub and K. O. Schäfer, *Z. Anorg. Allg. Chem.*, 1999, **625**, 1217.

16 M. Harvey, S. Baggio, R. Baggio and A. Mombrú, *Acta Crystallogr., Sect. C*, 1999, **55**, 1457.

17 M. Harvey, S. Baggio, L. Suescun and R. F. Baggio, *Acta Crystallogr., Sect. C*, 2000, **56**, 811.

18 (*a*) R. F. Baggio, S. Baggio, M. I. Pardo and M. T. Garland, *Acta Crystallogr., Sect. C*, 1996, **52**, 1939; (*b*) E. Freire, S. Baggio, L. Suescun and R. Baggio, *Aust. J. Chem.*, 2000, **53**, 785.

19 M. Harvey, S. Baggio, A. Mombrú and R. Baggio, *Acta Crystallogr., Sect. C*, 2000, **56**, 771.

20 A. Bondi, *J. Chem. Phys.*, 1964, **68**, 441.

21 (*a*) D. H. Smith and K. S. Seshadri, *Spectrochim. Acta, Part A*, 1999, **55**, 795; (*b*) K. Nakamoto, *Infrared and Raman Spectra of Inorganic and Co-ordination Compounds*, J. Wiley & Sns, New York, 3rd edn., 1978, p 134.

22 S. Xiao, T. Chen, B. Zhong, C. L. Stern and D. E. Ellis, *Acta Crystallogr., Sect. C*, 1999, **55**, 994.

23 W.-H. Leung, H. Zheng, J. L. C. Chim, J. Chan, W.-T. Wong and I. D. Williams, *J. Chem. Soc., Dalton Trans.*, 2000, 423.

24 I. Ghatak, D. M. P. Mingos, M. B. Hursthouse and K. M. A. Malik, *Transition Met. Chem.*, 1979, **4**, 260.

25 R. D. Shannon, *Acta Crystallogr., Sect. A*, 1976, **32**, 751.

26 (*a*) M. Ishaque Khan, S. Cevik and R. J. Doedens, *Inorg. Chim. Acta*, 1999, **292**, 112; (*b*) M. G. Hutchings, M. C. Grossel, D. A. S. Merckel, A. M. Chippendale, M. Kenworthy and G. McGeorge, *Cryst. Growth Des.*, 2001, **1**, 339; (*c*) R. Cini, D. G. Musaev, L. G. Marzilli and K. Morokuma, *J. Mol. Struct. (THEOCHEM)*, 1997, **392**, 55.

27 A. Arhar, L. Golic, V. Jordanovska and J. Siftar, *Bull. Slov. Chem. Soc.*, 1981, **28**, 311.

28 J. Habash, R. L. Beddoes and A. J. Smith, *Acta Crystallogr., Sect. C*, 1991, **47**, 1595.

29 P. J. Arnold, S. C. Davies, J. R. Dilworth, M. C. Durrant, D. V. Griffiths, D. L. Hughes, R. L. Richards and P. C. Sharpe, *J. Chem. Soc., Dalton Trans.*, 2001, 736.

30 P. O. Lumme, H. Knuuttila and E. Lindell, *Acta Crystallogr., Sect. C*, 1996, **52**, 51.

31 L. R. Rardin, W. B. Tolman and S. J. Lippard, *New J. Chem.*, 1991, **15**, 417.

32 T. C. Ullrich, M. Blaesse and R. Huber, *ATP Sulfurylase From S. Cerevisiae*, The PDB Protein Data Bank, Research Collaboratory for Structural Bioinformatics, The State University of New Jersey, the San Diego Supercomputer Center at the University of California, San Diego, and the National Institute of Standards and Technology, PDB-Code 1G8F, Deposition Date Nov 17, 2000.